

Article

Phenolic and Acidic Compounds in Radiation Fog at Strasbourg Metropolitan

Dani Khoury ^{1,2} , Maurice Millet ^{1,*}, Yasmine Jabali ² and Olivier Delhomme ^{1,3} 

¹ Institute of Chemistry and Processes for Energy, Environment and Health (UMR 7515 CNRS), University of Strasbourg, CEDEX 3, F-67087 Strasbourg, France; dani.khoury@anses.fr (D.K.); olivier.delhomme@univ-lorraine.fr (O.D.)

² Environmental Engineering Laboratory (EEL), Faculty of Engineering, University of Balamand, Kelhat-El Koura, Tripoli P.O. Box 100, Lebanon; yasmine.jabaly@balamand.edu.lb

³ University of Lorraine, F-57070 Metz, France

* Correspondence: mmillet@unistra.fr; Tel.: +33-(0)368-852-866

Abstract: Sixty-four phenols grouped as nitrated, bromo, amino, methyl, chloro-phenols, and cresols, and thirty-eight organic acids grouped as mono-carboxylic and dicarboxylic are analyzed in forty-two fog samples collected in the Alsace region between 2015 and 2021 to check their atmospheric behavior. Fogwater samples are collected using the Caltech Active Strand Cloudwater Collector (CASC2), extracted using liquid–liquid extraction (LLE) on a solid cartridge (XTR Chromabond), and then analyzed using gas chromatography coupled with mass spectrometry (GC-MS). The results show the high capability of phenols and acids to be scavenged by fogwater due to their high solubility. Nitro-phenols and mono-carboxylic acids have the highest contributions to the total phenolic and acidic concentrations, respectively. 2,5-dinitrophenol, 3-methyl-4-nitrophenol, 4-nitrophenol, and 3,4-dinitrophenol have the highest concentration, originating mainly from vehicular emissions and some photochemical reactions. The top three mono-carboxylic acids are hexadecenoic acid (C16), eicosanoic acid (C18), and dodecanoic acid (C12), whereas succinic acid, suberic acid, sebacic acid, and oxalic acid are the most concentrated dicarboxylic acids, originated either from atmospheric oxidation (mainly secondary organic aerosols (SOAs)) or vehicular transport. Pearson’s correlations show positive correlations between organic acids and previously analyzed metals ($p < 0.05$), between mono- and dicarboxylic acids ($p < 0.001$), and between the analyzed acidic compounds ($p < 0.001$), whereas no correlations are observed with previously analyzed inorganic ions. Total phenolic and acidic fractions are found to be much higher than those observed for pesticides, polycyclic aromatic hydrocarbons (PAHs), and polychlorinated biphenyls (PCBs) measured at the same region due to their higher scavenging by fogwater.

Keywords: Alsace; carboxylic acids; dicarboxylic acids; nitrophenols; atmospheric oxidation



Citation: Khoury, D.; Millet, M.; Jabali, Y.; Delhomme, O. Phenolic and Acidic Compounds in Radiation Fog at Strasbourg Metropolitan. *Atmosphere* **2024**, *15*, 1240. <https://doi.org/10.3390/atmos15101240>

Academic Editor: Daniel Beysens

Received: 2 September 2024

Revised: 14 October 2024

Accepted: 16 October 2024

Published: 17 October 2024



Copyright: © 2024 by the authors. Licensee MDPI, Basel, Switzerland. This article is an open access article distributed under the terms and conditions of the Creative Commons Attribution (CC BY) license (<https://creativecommons.org/licenses/by/4.0/>).

1. Introduction

Fog droplets can effectively scavenge gaseous and particulate water-soluble components from the atmosphere due to the large surface area of fog droplets [1]. Among these compounds, atmospheric phenols, particularly nitrophenols (NPhs), have gained significant attention due to their known toxicity to humans [2] and wildlife [3,4], as well as their suspected role in forest decline in Central and Northern Europe [5,6]. Leuenberger et al. (1988) demonstrated that dinitrophenols (DNPhs) can have toxic effects on plants at rain concentrations between 1 and 10 nM m^{−3}, inhibiting plant growth, nutrient assimilation, and transpiration [3,7]. Although some nitrated phenols are listed as priority pollutants by the Environmental Protection Agency (EPA), there has been limited data on their environmental concentrations since then [8]. Existing knowledge is mostly based on concentration data from rain [5,7,9–11], air [11–15], clouds [16], snow [17], and particulate matter [18]. A notable gap in the data is the occurrence of these organic pollutants in fogwater, where

high concentrations have been observed in preliminary studies [6,19]. The low air–water partition coefficients of NPHs make them one of the most prevailing families accumulated in fogwater [20]. NPHs were detected in snow and lake water in Antarctica's Terra Nova Bay, with possible explanations including local atmospheric chemistry and photochemical processes involving nitrate (NO_3) and nitrite (NO_2) [21]. The measured ambient concentration of NPHs (phenol, 2-NPh, 4-NPh, and 2,4-DNPh) showed considerable variability among different matrices (rain, cloud, and fog). The concentrations of phenol, 4-NPh, and 2,4-DNPh reached higher values than those detected in the gas phase, rain, cloud, and snow. For instance, phenol was detected in fog up to $91.8 \mu\text{g L}^{-1}$ compared to 0.4, 5.4, and $7.7 \mu\text{g L}^{-1}$, respectively, in the gas phase, cloud, and rain. 2-NPh was detected in all matrices except fogwater at levels reaching up to $1.4 \mu\text{g L}^{-1}$. The concentration of 4-NPh was the highest in fog (up to $88 \mu\text{g L}^{-1}$), followed by cloud (up to $21 \mu\text{g L}^{-1}$), rain (up to $16 \mu\text{g L}^{-1}$), and gas phase (up to $0.3 \mu\text{g L}^{-1}$). 2,4-DNPh had the highest concentration in fog (up to $30.4 \mu\text{g L}^{-1}$), followed by cloud (up to $5.4 \mu\text{g L}^{-1}$), rain (up to $5.0 \mu\text{g L}^{-1}$), and gas phase (up to $0.08 \mu\text{g L}^{-1}$). The reasons behind that can be explained by the fact that smaller droplets of fog can more efficiently capture organic compounds and remain in the atmosphere for longer periods. This extended residence time allows for the accumulation of products from liquid phase processes, further influencing nitrophenol levels [22].

Phenolic compounds may exist in both phases, gaseous and aqueous, and their distribution is a complex phenomenon not easily described by simple gas/liquid equilibrium models [16]. They can be directly emitted through combustion processes, particularly from vehicles [18,23–26] and diesel engines [27,28], as well as coal and wood, and through the production of dyes, drugs, explosives, disinfectants, and pesticides [29]. Significant emissions may also come from the plastic and chemical industries and paper manufacturing, where such compounds are used extensively for wood protection [30,31]. Indirect emissions of atmospheric phenols and NPHs are often much higher than what could be attributed solely to direct emissions, indicating the potential for secondary aerosol formation (SOAs) through reactions involving volatile aromatic compounds (VOCs) in the atmosphere, either in the gas or condensed phases. The direct photolysis of NPHs leading to the formation of SOAs was studied for the first time in a quartz glass simulation chamber exposed to simulated solar radiation. The findings demonstrated that SOA forms quickly. The suggested mechanism for the gas phase degradation of NPHs via photolysis involved the generation of biradicals, which may further react with oxygen to produce low-volatility and highly oxygenated compounds that contribute to the formation of SOAs [32]. One of the primary processes responsible for the formation of NPHs is the nitration of phenol, which can occur in both phases in the presence of hydroxyl (OH) and nitrate (NO_3) radicals. Another route of atmospheric NPHs and other compounds is the photochemical oxidation of benzene and toluene [33–38]. It has been estimated that atmospheric formation processes contribute to more than one-third of NPHs in the environment. The formation of phenols and NPHs through their reactions with OH and NO_3 radicals has been previously investigated by many researchers [39–44]. The rapid gas phase reaction of NO_3 radicals with phenol produced 2-nitrophenol as the sole significant nitration product. However, when ozone is present, considerable amounts of 4-nitrophenol and p-benzoquinone are also generated [41]. For instance, it has been shown that the oxidation of aromatic compounds in the gas phase contributes mainly to NPHs in the oil and gas industry located in the US [42]. In another study, it was observed that 6-methyl-2-nitrophenol (6-M-2-NPh) is a primary product in reactions of o-cresol with both OH and NO_3 radicals [40].

Moreover, organic acids are widely present in the atmosphere [45], and they have been observed in the gas phase, aqueous phase, and aerosols [46–49]. A wide range of organic acids can be found in the troposphere and act as cloud condensation nuclei due to their high polarity and hygroscopicity [50]. Their concentrations vary significantly in the different phases across urban, marine, rural, and polar regions [45,51,52]. For instance, Kawamura et al. (1985) detected gaseous C1–C10 alkanic acids in the atmosphere of Los Angeles, with formic acid and acetic acid being the most abundant, reaching levels of several

parts per billion by volume (ppbv), followed by propanoic acid at around 0.1 ppbv [53]. In Japan, Satsumabayashi et al. (1989) measured acetic acid, propanoic acid, and butyric acid at concentrations of 4.0–8.0, 0.3–0.7, and 0.1–0.3 ppbv, respectively [54]. Formic acid, propanoic acid, and acetic acid were also quantified in tropospheric snow, fogwater, rainwater, cloud water, and even polar ice samples [55]. In contrast to monocarboxylic acids (MCA), which are more volatile, dicarboxylic acids (DCA) tend to exist in the atmosphere primarily in particulate form [56]. Common organic acids in atmospheric particulates include malonic, maleic, oxalic, succinic, and phthalic acids, as identified in previous field studies across urban and rural areas of Southeast and East Asia, Central Europe, Africa, the United States, marine regions, and the Arctic [57–60].

Organic acids originate from direct anthropogenic emissions, including vehicle exhaust, fossil fuel combustion, and biomass burning [53,61–64], biogenic emissions, including plants, bacteria and microorganisms, soil, and ants [48,64–68], and in situ production from atmospheric precursors [68–70]. Photochemical formation is a source of organic acids, especially during summer [71,72]. Veres et al. (2011) demonstrated that organic acids could be rapidly generated through photooxidation reactions in the urban atmosphere of Pasadena [59]. Similarly, Mattila et al. (2018) detected formic, propanoic, butyric, valeric, and pyruvic acids in the Colorado Front Range atmosphere. Their studies showed that direct emissions from transportation, agricultural activities, and photochemical oxidation are the primary sources of these acids in the atmosphere based on correlations between atmospheric tracers and the investigated compounds [73]. The most common organic acids that have been previously detected in fogwater are formic and acetic acids as MCA [74–76] and oxalic and succinic acids as DCA [77–79].

The concentrations of both phenols and organic acids in fogwater exhibit spatio-temporal variability. These variations are influenced by seasonal changes in biogenic emissions [57,64,65,74,80,81], daily fluctuations in anthropogenic sources and photochemical reactions [57,63,64,82–88], and convective mixing of air from higher altitudes [89]. In polluted areas, their atmospheric levels are typically higher, but their stability facilitates their global dispersion. That is why NPhs were detected at important levels in remote regions, as in the case of the summit of Great Dun Fell in Northern England [22].

Fog sampling started in Alsace at the beginning of the 1990s [90–93], and it continued until the end of the 1990s [94]. Lately, fogwater sampling has been restarted to analyze its inorganic (ions and heavy metals) and organic matters (including polycyclic aromatic hydrocarbons (PAHs), polychlorinated biphenyls (PCBs), and pesticides) at different sites in the region between 2015 and 2021 [95–97]. In the current study, 64 phenols, including chloro-, di-, and trichlorophenols (CPhs, DCPhs, and TCPhs, respectively), bromo- and dibromophenols (BPhs and DBPhs, respectively), aminophenols (APhs), phenol/cresols, and nitro-, dinitro-, and methylnitrophenols (NPhs, DNPhs, and MNPhs, respectively), and 38 organic acids (MCA and DCA) are measured for the first time in fogwater samples collected at Strasbourg metropolitan. The global objective of this study is to determine the abundant compounds scavenged by fog droplets and to assess their emission sources. It is worth mentioning that only once, twelve phenols were analyzed in fog samples taken from Northeastern Bavaria in Germany [19], while only a few organic acids were analyzed in fog samples at the mountain site of Hokkaido in Japan [98]. This shows the importance and originality of this study to better understand their occurrence and fate in the atmosphere.

2. Materials and Methods

2.1. Fogwater Sampling

Forty-two radiation fogwater samples were collected at four sites (Cronenbourg, Strasbourg, Geispolsheim, and Erstein) in the Alsace region (Northeastern France) during 2015, 2016, 2017, 2018, and 2021. The volume of the collected samples varied between 25 to 248 mL depending on the duration and density of foggy event. The urban site, Strasbourg, surrounds the three other sites, which are located in its northwest, west, and southwest (see Figure S1 and Table S1 in the Supplementary Materials). The sampling sites are

located near sources of heavy pollution, including industrial areas (bordering Strasbourg), unconventional residential heating (such as wood burning), steel and aluminum factories, agricultural activities (particularly in Geispolsheim), and vehicle emissions from the major highway. This region is well known for its radiation fog that appears during nighttime and disappears in the early morning. The duration of foggy events, on average, is six hours. The condensation of fog droplets occurs on the inclined strands of the Caltech Active Strand Cloudwater Collector (CASC2), where they are collected in a glass bottle, as described elsewhere [99,100]. After collection, on-site filtration and measurements are directly performed to measure the conductivity and pH of the sample. The latter is divided into different aliquots to analyze its inorganic [95] and organic fractions as well as its dissolved organic carbon (DOC) [96,97]. The samples are then stored at $-18\text{ }^{\circ}\text{C}$ until extraction.

2.2. Fogwater Extraction and Analysis

Fog samples were extracted using liquid–liquid extraction (LLE) performed on a solid support (XTR Chromabond), as described in Khoury et al. (2023) [101]. Briefly, it is based on loading 50 mL of the collected fog volume on the support, waiting 15 min to flow down the column, and eluting successively with 40 mL of dichloromethane and 40 mL of ethyl acetate. This was followed by the reconcentration of the collected extract to 1 mL gently under the fume hood. The latter was derivatized with 50 μL of *N-tert*-Butyldimethylsilyl-*N*-methyltrifluoroacetamide (MtBSTFA) for 1 h at $80\text{ }^{\circ}\text{C}$ to convert phenols and acids to more volatile and more stable compounds and then the extract was injected into the analytical instrument. In case the fog volume was higher than 50 mL, two extractions were executed and analyzed separately. In case fog volume was lower than 50 mL, then the sample was re-constituted with ultrapure water to 50 mL. The validation parameters for the analyzed phenols and acids are found in Tables S2–S4 in the Supplementary Materials.

A gas chromatography–mass spectrometry (GC-MS) Trace GC ultra/ISQ II in the selected ion monitoring (SIM) mode equipped with a single quadrupole was used for the analysis of phenols and acids. The GC column was the XLB of $60\text{ m} \times 0.25\text{ mm i.d} \times 0.25\text{ }\mu\text{m}$ film thickness. The injection was performed in the splitless mode at $250\text{ }^{\circ}\text{C}$ for 1 min. The transfer line and source temperatures were $300\text{ }^{\circ}\text{C}$ and $210\text{ }^{\circ}\text{C}$, respectively. The carrier gas was Helium (purity $> 99\%$), flowing at a rate of 1 mL min^{-1} . For phenols, the initial oven temperature was set at $50\text{ }^{\circ}\text{C}$ for 4 min, followed by a ramp to $160\text{ }^{\circ}\text{C}$ at a rate of $40\text{ }^{\circ}\text{C min}^{-1}$, then followed by a ramp to $180\text{ }^{\circ}\text{C}$ at a rate of $5\text{ }^{\circ}\text{C min}^{-1}$, followed by a linear ramp to $240\text{ }^{\circ}\text{C}$ at a rate of $3.2\text{ }^{\circ}\text{C min}^{-1}$, then followed by a ramp to $300\text{ }^{\circ}\text{C}$ at a rate of $10\text{ }^{\circ}\text{C min}^{-1}$, where it was kept for 12 min. The total run time was 46.5 min. For acids, the initial oven temperature was set at $50\text{ }^{\circ}\text{C}$ for 3 min, followed by a ramp to $160\text{ }^{\circ}\text{C}$ at a rate of $45\text{ }^{\circ}\text{C min}^{-1}$, then followed by a ramp to $270\text{ }^{\circ}\text{C}$ at a rate of $7\text{ }^{\circ}\text{C min}^{-1}$, then followed by a ramp to $330\text{ }^{\circ}\text{C}$ at a rate of $15\text{ }^{\circ}\text{C min}^{-1}$ where it was kept for 17 min. The total run time was 45.15 min [101]. Under those analytical and instrumental conditions, the extraction protocol yields high resolution peaks on the chromatograms in a way that all compounds are well analyzed with very high intensity (see Figure 1).

Field blanks, gathered on-site during the washing step of fog collection, as well as laboratory blanks (during extractions and injections), are performed continuously to check the contamination levels, if any, during the analysis of fog samples. All blanks are treated in the same way as real samples.

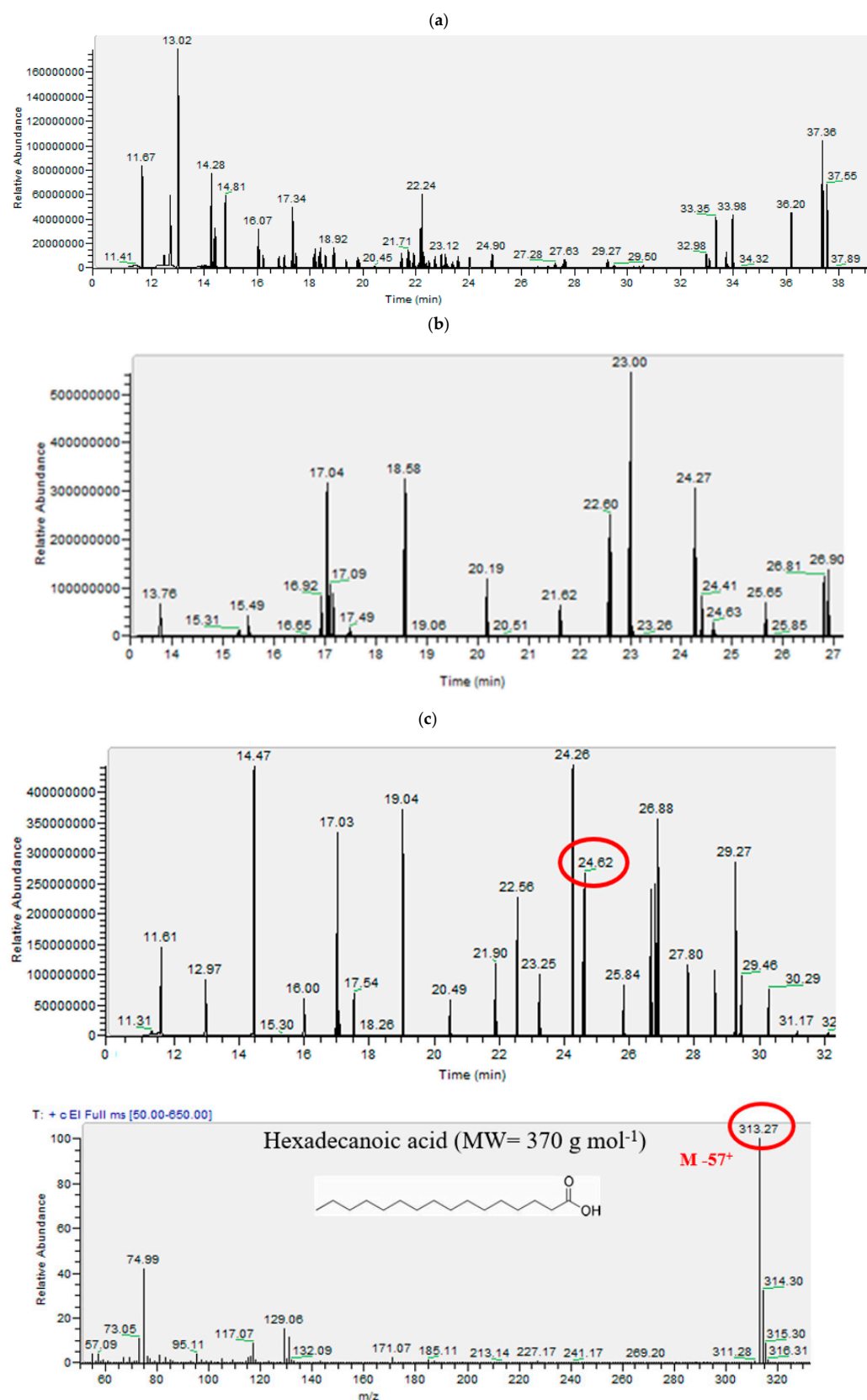


Figure 1. Chromatograms for (a) phenols, (b) DCA, and (c) MCA (followed by an example of the mass spectrometer after the derivatization of hexadecanoic acid) in the selection ion monitoring mode (SIM).

3. Results and Discussions

3.1. Phenols

3.1.1. Individual Phenols Concentration and Detection in Fog Samples

Thirty-five out of the sixty-four analyzed phenols are detected in fog samples. The median detection frequencies (DFs) for phenolic compounds across all sites show that many compounds are consistently present, with several reaching a detection frequency of 100%. These include 2,5-DCPh, PCPh, 2,3,4-TCPh, 5-M-2-NPh, 4-M-2-NPh, 4-NPh, and multiple DNPhs. This suggests that these compounds are commonly detected across all investigated sites and may reflect widespread contamination. On the other hand, compounds such as 4-CPh and 2,4,6-TCPh show much lower median detection frequencies (2% and 4%, respectively), indicating they are less frequently detected. Phenol itself has a moderate median detection frequency of 76%, showing that it is detected consistently but not as universally as some other phenolic compounds (o/p-cresol). This analysis suggests variability in the presence of phenolic compounds, with certain compounds being far more ubiquitous across the sampled sites.

Figure 2 shows the concentrations and contributions of phenol/cresols, BPhs, APhs, CPhs, NPhs, and the rest of the phenols, allowing a clear comparison of levels across sites. The graph illustrates that NPhs dominate the occurrence across all locations, with values around 63–70% (average of 66%) of the total phenol content. They also have the highest median concentrations at all sites, ranging between 16.9 and 27.0 $\mu\text{g L}^{-1}$ (average of 22.1 $\mu\text{g L}^{-1}$). This suggests that they are the most prevalent phenolic compounds in the region, which can be attributed to industrial or environmental factors specific to this region. Their median concentrations vary in the range of 14.3–21.9 $\mu\text{g L}^{-1}$ (average of $18.2 \pm 3.2 \mu\text{g L}^{-1}$), 9.9–23.4 $\mu\text{g L}^{-1}$ (average of $15.8 \pm 6.8 \mu\text{g L}^{-1}$), 11.4–38.9 $\mu\text{g L}^{-1}$ (average of $25.2 \pm 19.5 \mu\text{g L}^{-1}$), and 18.5–20.6 $\mu\text{g L}^{-1}$ (average of $19.6 \pm 1.5 \mu\text{g L}^{-1}$), respectively, at Geispolsheim, Erstein, Strasbourg, and Cronenbourg. Phe/cresols show a moderate contribution across locations, ranging from 6% to 13% (average of 10%), with median levels varying from 2.2 to 3.8 $\mu\text{g L}^{-1}$ (average of 3.2 $\mu\text{g L}^{-1}$). Thus, they make up a smaller portion of the total phenolic content. BPh, APh, and CPh have relatively small percent contributions, typically below 10%, with average concentration levels below 2 $\mu\text{g L}^{-1}$.

3.1.2. NPhs Detected in Fog Samples

Distribution Across Sites

Figure 3 illustrates the boxplots showing the concentration distribution of various nitrophenols across different sites. The box indicates the range in which the middle 50% of all data lies. The lower and upper ends are the first (25th percentile) and third quartile (75th percentile), respectively, and in between is the interquartile range (length of the box). The two ends of the external bar show the minimum and maximum observation. The solid line indicates the median values (50th percentile); it shows the central point where 50% of the values lie below it and 50% lie above it. Individual data points that fall outside the whiskers meaning they are far from the typical range of the data, are considered extreme values or outliers (such as the most contaminated samples for each compound).

At Geispolsheim, 2-NPh exhibits moderate concentrations with some variability, reflected in the wide spread of the data and a few outliers indicating occasional spikes in pollution. Erstein shows more stable and lower levels, with fewer outliers, suggesting more consistent contamination. Cronenbourg has slightly higher concentrations than Erstein but still shows some variability and outliers, pointing to sporadic contamination events. Strasbourg exhibits a similar pattern to Geispolsheim, with moderate concentrations, occasional variability, and a few outliers, suggesting periodic contamination at this site. At Geispolsheim, 4-NPh has moderate concentrations with considerable variability and a few outliers, suggesting periodic industrial discharges. Erstein shows slightly higher median concentrations with moderate variability and few outliers, pointing to steady contamination levels. Cronenbourg exhibits the lowest concentrations with a narrow spread, indicating stable and lower contamination levels. Strasbourg has the highest concentration levels

with significant variability and some outliers, suggesting a higher degree of industrial contamination and periodic pollution events. At Geispolsheim, 3-M-2-NPh concentrations are moderate, with a few outliers indicating sporadic contamination. Erstein shows slightly lower levels but with more variability and outliers, suggesting less stable pollution sources. Cronenbourg exhibits the lowest concentrations with a narrow spread, indicating stable contamination levels over time. Strasbourg shows moderate concentrations with a bit more variability and occasional outliers, reflecting periodic contamination similar to Geispolsheim. At Geispolsheim, 5-M-2-NPh shows moderate concentrations with some variability and occasional outliers, pointing to irregular contamination. Erstein has slightly higher concentrations with more variability and several outliers, indicating fluctuating contamination levels. Cronenbourg shows the lowest concentrations with a stable spread, suggesting consistent and low contamination. Strasbourg shows moderate concentrations with wide variability and several outliers, implying periodic contamination spikes similar to Erstein. At Geispolsheim, 4-M-2-NPh shows moderate concentrations with considerable variability and a few outliers, indicating periodic contamination. Erstein has slightly higher concentrations with similar variability, pointing to steady but fluctuating contamination. Cronenbourg exhibits lower concentrations with more stable contamination patterns and fewer outliers, indicating more consistent levels. Strasbourg shows moderate concentrations with significant variability and outliers, suggesting more irregular contamination events similar to Geispolsheim. At Geispolsheim, 2,5-DNPh shows moderate concentrations but significant variability, with many outliers suggesting periodic high pollution levels. Erstein has slightly higher concentrations with even more variability and numerous outliers, indicating fluctuating contamination events. Cronenbourg exhibits more stable and lower concentrations with fewer outliers, suggesting minimal sporadic contamination. Strasbourg shows moderate concentrations similar to Geispolsheim, with wide variability and frequent outliers, indicating periodic high levels of contamination. At Geispolsheim, 3-M-4-NPh exhibits moderate concentrations with considerable variability and a few outliers, indicating irregular contamination events. Erstein shows slightly higher concentrations with more variability and some outliers, suggesting fluctuating contamination levels. Cronenbourg has lower and more stable concentrations, as indicated by the narrow spread, with few outliers reflecting a more consistent contamination pattern. Strasbourg exhibits the highest concentrations for 3-M-4-NPh with significant variability and several outliers, indicating periodic high contamination events, likely from industrial or urban sources. At Geispolsheim, 3,4-DNPh shows moderate concentrations with a fair amount of variability and a few outliers, suggesting occasional spikes in contamination levels. Erstein has slightly higher concentrations but with more variability and several outliers, indicating irregular and fluctuating contamination sources. Cronenbourg exhibits lower concentrations with a more stable spread and fewer outliers, pointing to a consistent and lower level of contamination. Strasbourg shows moderate concentrations, with a relatively wide spread and a few outliers, suggesting periodic high contamination events similar to Geispolsheim and Erstein. At Geispolsheim, 2,6-DNPh exhibits low to moderate concentrations with some variability but few outliers, indicating relatively stable contamination levels. Erstein shows slightly higher concentrations with a wider spread, suggesting more variability and potential contamination spikes. Cronenbourg exhibits lower concentrations with a narrow spread, reflecting stable contamination patterns and few outliers. Strasbourg shows moderate concentrations with some variability and occasional outliers, pointing to periodic high contamination events but overall consistent levels. At Geispolsheim, 2,4-DNPh shows low to moderate concentrations with minimal variability and few outliers, indicating stable contamination. Erstein has slightly higher concentrations with moderate variability, pointing to a more variable contamination pattern. Cronenbourg exhibits the lowest concentrations with stable levels and no significant outliers, indicating minimal contamination from this compound. Strasbourg shows moderate concentrations with some variability but few outliers, suggesting consistent contamination with occasional spikes. 2,4-DNPh has a tighter distribution with less variance, indicating more consistent concentrations across

sites. At Geispolsheim, 3,4-DNPh shows moderate concentrations with some variability and occasional outliers, indicating periodic spikes in contamination. Erstein exhibits higher concentrations with more variability and a few outliers, suggesting irregular contamination events. Cronenbourg has lower concentrations with minimal variability, indicating stable contamination levels. Strasbourg shows moderate concentrations with some variability and a few outliers, pointing to periodic contamination but overall consistent levels. At Geispolsheim, 2-M-3-NPh exhibits moderate concentrations with some variability and a few outliers, suggesting occasional contamination spikes. Erstein shows slightly lower concentrations with less variability and few outliers, reflecting more stable contamination. Cronenbourg has the highest concentrations for this compound but with a consistent spread and fewer outliers, indicating stable contamination patterns. Strasbourg shows moderate concentrations with a wider spread and some outliers, suggesting periodic contamination events but overall consistent levels.

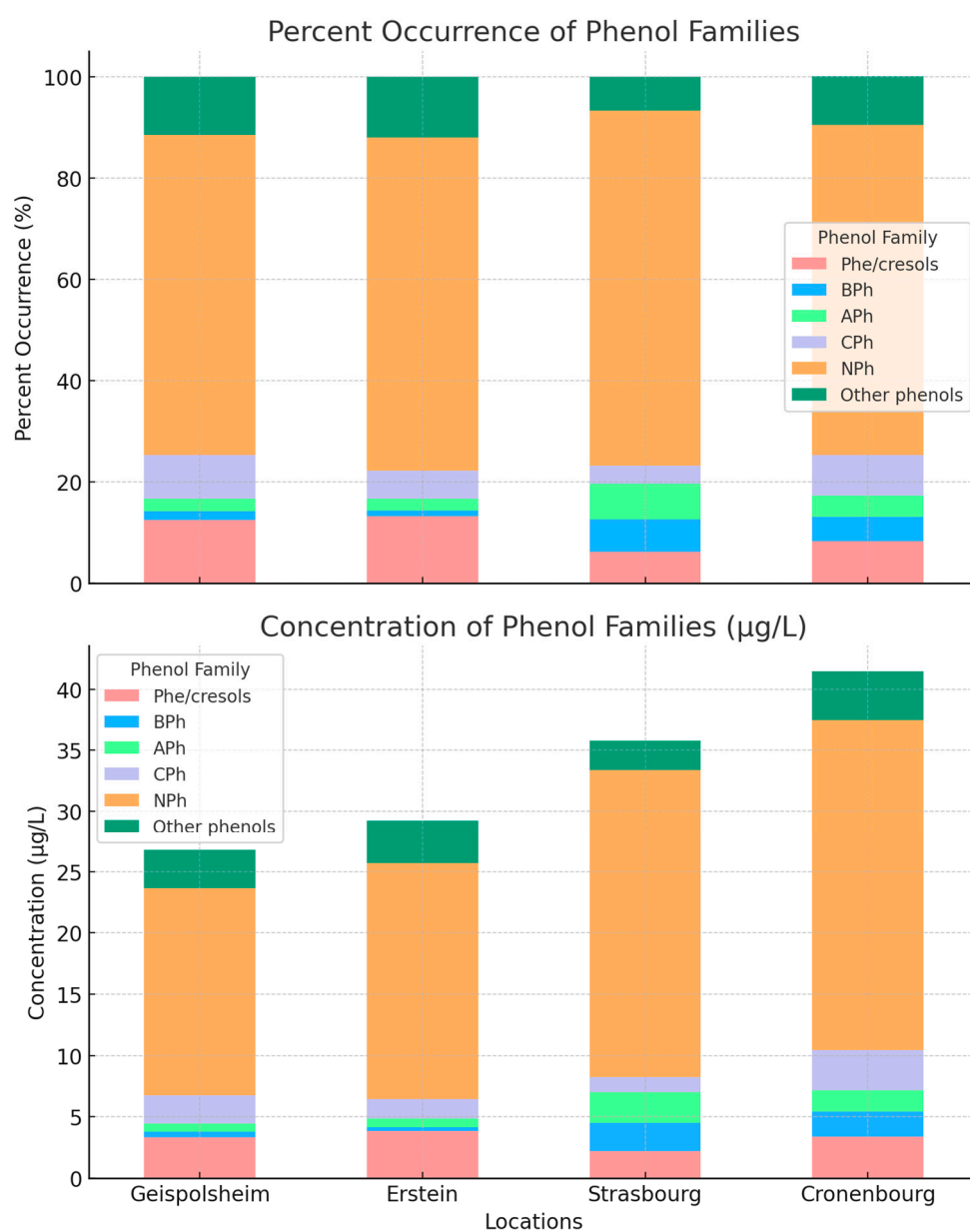


Figure 2. Concentration (**lower**) and contributions (**upper**) of the different phenolic families across all sites.

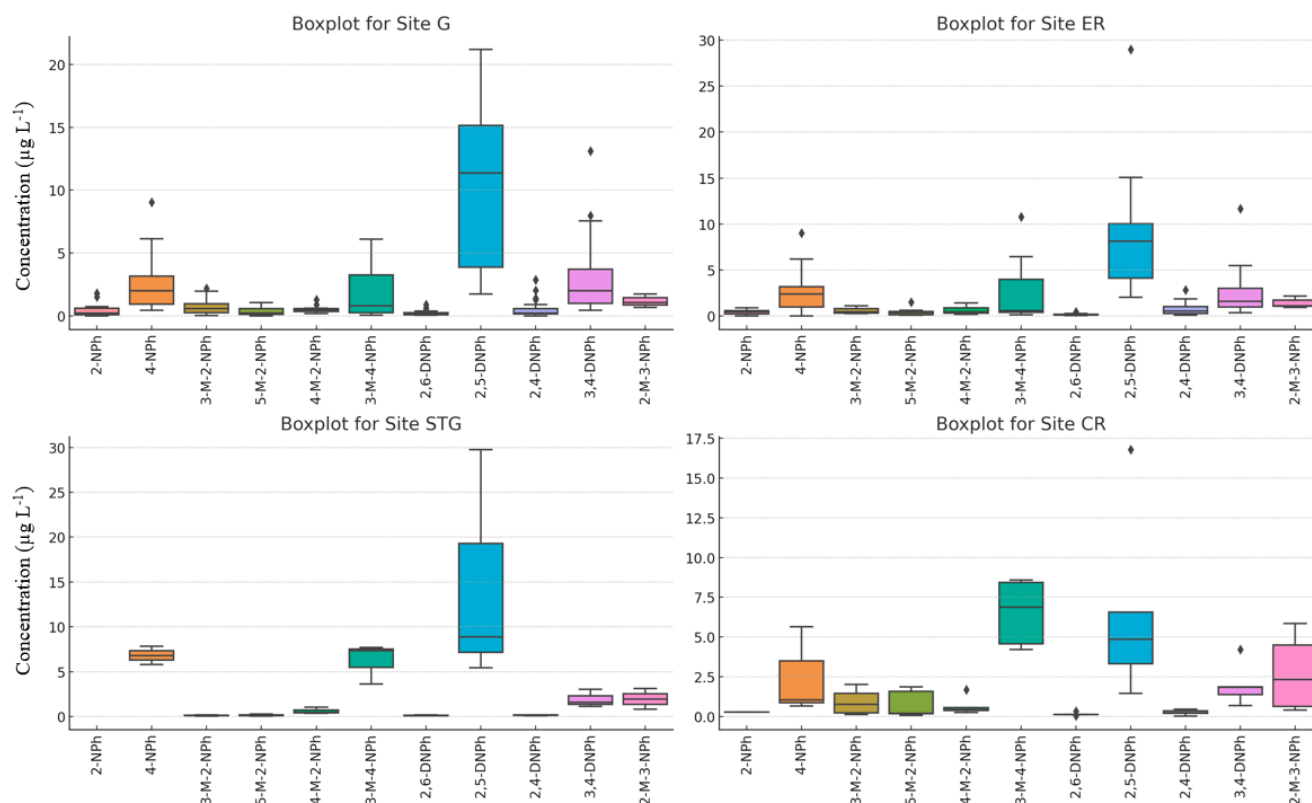


Figure 3. Boxplots of NPhs at the four locations over the whole sampling period. G: Geispolsheim, ER: Erstein, STG: Strasbourg, CR: Cronenbourg.

Overall, the plot reveals that 2,5-DNPh, 3-M-4-NPh, 4-NPh, and 3,4-DNPh have the highest contamination levels in Alsace, whose median concentrations are, respectively, 8.9, 2.7, 2.1, and 1.8 $\mu\text{g L}^{-1}$. Geispolsheim and Erstein are predominantly contaminated by 2,5-DNPh and 4-NPh, whose median concentrations are 11.4 and 8.1 $\mu\text{g L}^{-1}$, and 2.1 and 2.4 $\mu\text{g L}^{-1}$, respectively. 4-NPh and 3,4-DNPh almost have the same levels at both sites (median of 2.1 and 2.0, respectively). Cronenbourg and Strasbourg are found to be more contaminated by 3-M-4-NPh and 2,5-DNPh, whose median concentrations are, respectively, 6.9 and 7.3 $\mu\text{g L}^{-1}$, and 4.9 and 8.9 $\mu\text{g L}^{-1}$. 4-NPh is also observed at high concentration at Strasbourg (median of 6.8 $\mu\text{g L}^{-1}$) as well as 2-M-3-NPh (median of 2.0 $\mu\text{g L}^{-1}$). At the same time, Cronenbourg is found to be further contaminated by 3,4-DNPh (median of 1.8 $\mu\text{g L}^{-1}$) and 2-M-3-NPh (median of 2.3 $\mu\text{g L}^{-1}$). 2,5-DNPh or 4-NPh exhibit a higher spread with more variability in their values across the sites. This could indicate that certain compounds are more sensitive to environmental or site-specific factors.

ANOVA test is applied to check if the observed differences are statistically different. The results show that for all compounds, except for 3-M-4-NPh, the p -values are greater than 0.05, meaning that the differences across sites are not significantly different. Additionally, Pearson's correlation shows strong correlations between 3-M-2-NPh and 5-M-2-NPh (0.64, $p < 0.05$) and 3-M-4-NPh and 4-NPh (0.61, $p < 0.05$) showing their co-occurrence in the atmosphere and their influence by the same processes and sources (breakdown of similar organic compounds, etc.). Moderate correlations are found between 5-M-2-NPh and 4-M-2-NPh (0.46, $p < 0.05$) and 2-NPh and 5-M-2-NPh (0.55, $p < 0.05$), suggesting some correlations possibly due to similar sources within the environmental medium.

As a conclusion, Geispolsheim and Strasbourg show moderate to high contamination levels across most compounds, with significant variability and frequent outliers, indicating irregular contamination likely from industrial or urban sources. Erstein generally has slightly higher contamination levels but with more variability and frequent spikes, suggest-

ing fluctuating pollution. Cronenbourg consistently shows the lowest concentrations with stable patterns, indicating less contamination or more regulated sources.

Sources of Atmospheric NPhs

The formation of NPhs in the combustion processes of motor vehicles has been reported in previous studies in the exhaust gas of car engines in the range of mg m^{-3} . The combustion of coal and wood also lead to their introduction into the atmosphere. Traffic activity is most likely to be one of the main sources of these compounds in the atmosphere, either directly or indirectly, via further atmospheric chemistry of traffic-emitted precursors. Direct traffic emission is likely to be an important source of NPhs in urban areas. Nitrated phenols may also enter the atmosphere through the intensive use of herbicides and insecticides in agriculture. Pesticides are susceptible to photochemical decomposition and hydrolysis reactions that mainly release 4-NPh. The latter is found to have the highest concentration in this study among the mono-NPhs. For instance, the ratio of 4-NPh to 2-NPh is higher than 1 in all fog samples (reaching very high values in some cases), which is somehow surprising because vehicle exhaust emits more 2-NPh than 4-NPh [22,26]. 3-NPh is not detected in any of the fog samples since its formation is unlikely in the atmosphere [19]. However, 2-NPh is detected in more than half of fog samples but at lower concentrations than 4-NPh. 2-NPh is known to be produced from the nitration of phenol in aqueous media and during photochemical nitration of aromatics in the air [33]. The primary reason behind its absence or low detection in fogwater could be attributed to its high Henry's law constant compared to 4-NPh [20]. Regarding DNPhs, the photochemical reaction of C_6H_6 with NO_x in the gaseous phase may yield 2,4-DNPh, 3,4-DNPh, 2,5-DNPh, and 2,6-DNPh [30]. 3-M-4-NPh is one of the main products of the photochemical reaction of $\text{C}_6\text{H}_5\text{CH}_3$ with NO_x . The levels of NPhs in fogwater are often significantly higher than might be expected from their whole direct emission sources, suggesting the possibility of secondary formation through reactions of aromatic compounds in the atmosphere, either in the gas phase or in the condensed phase.

3.1.3. Other Compounds Detected in Fog Samples

Figure 4 illustrates the boxplot of phe/cresols, APhs, CPhs, and BPhs across all sites. The boxplot suggests that phenol appears only sporadically across the sites. It is either absent or present at very low concentrations in fogwater, which could indicate limited local sources or rapid degradation in the atmosphere. The absence of a wider distribution may suggest that phenol concentrations are highly localized or episodic. Phenol is very reactive in the atmosphere formed during combustion processes or wastewater evaporation and thus different concentration levels can be expected at the investigated sites [102]. It has the highest concentrations at Erstein and Geispolsheim due to the emissions released from chemical industries that are located outside Strasbourg and in proximity to these two sites. Higher levels of o/p-cresols (mean of $2.0 \mu\text{g L}^{-1}$) than m-cresol (mean of $0.56 \mu\text{g L}^{-1}$) have been detected at all sites. Indeed, o-cresol is primarily used as a raw material for the manufacturing of herbicides in the Alsace region, which is characterized by its intensive farming and herbicide production. The distribution of m-cresol shows variability across different sites. There is limited variability in m-cresol concentrations at all sites, possibly due to its consistent sources or atmospheric conditions that limit its dispersion. There is minimal presence of outliers, indicating that m-cresol concentrations remain fairly stable in this environment and are not subjected to large-scale events. However, the distribution of o/p-cresol is broader with greater variability between sites. This suggests that it is more influenced by local emissions or atmospheric conditions. Other compounds including TCPhs, APhs, and BPhs are found at trace levels across all sites. The variabilities of most of them are relatively very small suggesting a steady and stable presence in the atmosphere. In some cases, 2-APh exhibits a large range, showing little fluctuation in its levels between sampling events across the same site.

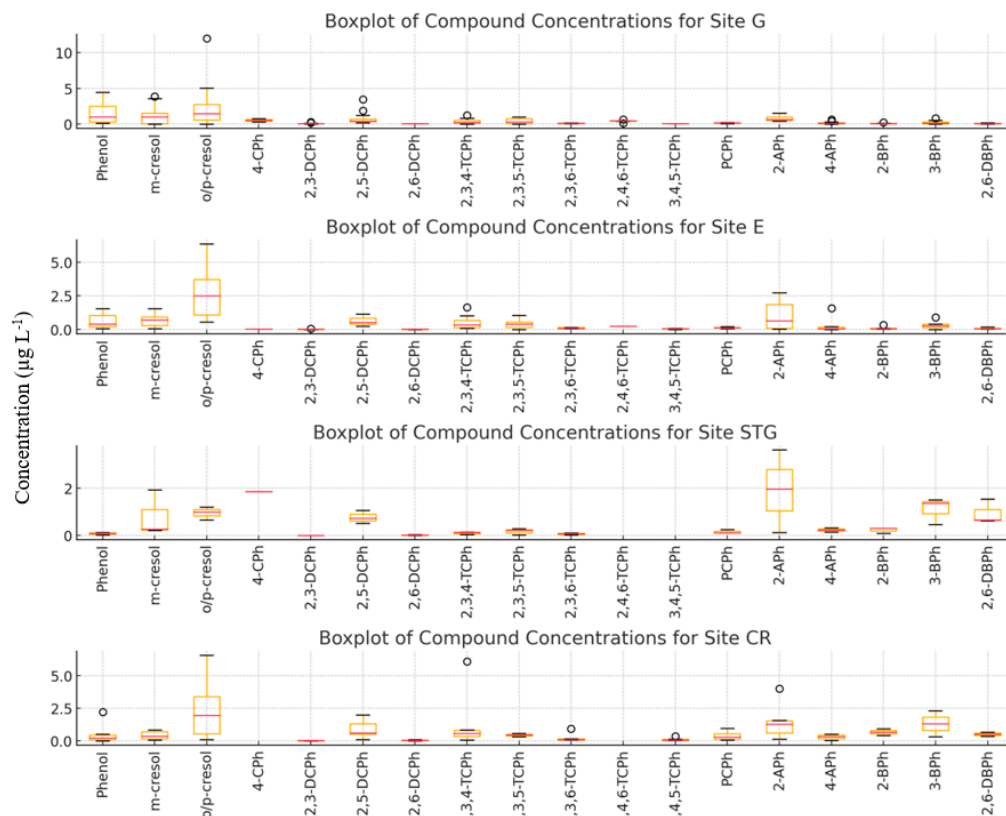


Figure 4. Boxplots of concentration levels ($\mu\text{g L}^{-1}$) for phe/cresols, APhs, CPhs, and BPhs across the four sites. G: Geispolsheim, ER: Erstein, STG: Strasbourg, CR: Cronenbourg.

3.1.4. Total Phenolic Concentrations

Strasbourg and Cronenbourg have the highest phenol levels (nearly the same) followed by Geispolsheim and Erstein. Their average concentrations are, respectively, 35.8 ± 19.5 , 31.7 ± 4.5 , 26.6 ± 3.4 , and $24.8 \pm 10.4 \mu\text{g L}^{-1}$. It is not surprising that the global concentrations are the highest at Strasbourg and Cronenbourg, since one of the major emissions is road traffic, which is more important than the other two sampling sites [15]. The total phenolic levels reported in this study are much higher than those previously observed for pesticides, PAHs, and PCBs [96,97]. The reason behind that is that phenols have higher hygroscopicity than others, leading to their better scavenging by fogwater. The total phenol concentrations in fogwater varied notably across the four sites, displaying different trends over the years. Geispolsheim experienced fluctuating levels, beginning with a decrease from $24.5 \mu\text{g L}^{-1}$ in 2015 to $23.2 \mu\text{g L}^{-1}$ in 2016, followed by a sharp increase to $29.5 \mu\text{g L}^{-1}$ in 2017. However, this upward trend leveled off in 2018 with a slight drop to $28.7 \mu\text{g L}^{-1}$. In contrast, Erstein demonstrated a significant increase, rising from $20.2 \mu\text{g L}^{-1}$ in 2015 to $25.7 \mu\text{g L}^{-1}$ in 2016, and spiking dramatically to $41.7 \mu\text{g L}^{-1}$ by 2018, marking one of the steepest rises observed. Similarly, Strasbourg saw a remarkable surge in phenol concentrations, from $22.1 \mu\text{g L}^{-1}$ in 2016 to an all-time high of $49.6 \mu\text{g L}^{-1}$ in 2018, the highest recorded across all sites. Cronenbourg, for which data are only available from 2018 onwards, showed a substantial increase from $28.5 \mu\text{g L}^{-1}$ in 2018 to $45.4 \mu\text{g L}^{-1}$ by 2021 (COVID-19 confinement period), following a rising trend similar to Strasbourg. These increases suggest a growing accumulation of phenols in fogwater across several sites, particularly between 2016 and 2018, with some variability in Geispolsheim's trends. There are no clear explanations that can describe the different trends because many of the phenolic levels are a function of many factors such as formation reactions in fog reservoirs, environmental conditions, anthropogenic emissions, Henry's coefficient, etc. [103]. This is in contrast with a study that analyzed phenols in rainwater samples at Strasbourg and

Erstein during 2002 and 2003 [104]. In their study, almost similar phenolic levels have been detected in both years supported by the unchangeable observations between both years neither in climate (temperature, rain, etc.), nor in traffic or industries that could affect their atmospheric emission levels. As an inter-individual comparison, the levels of 2,5-DNPh are always the most abundant in all fog samples at all times.

3.1.5. Comparison of Phenols with a Previous Study

The concentration ranges and median values for 4-NPh, 2,4-DNPh, and 3-M-4-NPh from our dataset are compared with the observations from a study performed in North-eastern Bavaria (Germany) during the autumn of 1988. The concentrations of 4-NPh in our dataset are generally lower, with the maximum value in this study ($9.04 \mu\text{g L}^{-1}$) falling within the lower end of the range reported in Bavaria. This suggests lower contamination levels at our sites compared to Bavaria in 1990. The concentrations of 2,4-DNPh in our dataset are significantly lower than the levels observed in Bavaria, with both the maximum and median values falling well below the Bavarian range. This indicates a much lower presence of this compound in our studied sites. The concentration range for 3-M-4-NPh in our dataset is comparable to that observed in Bavaria, with the maximum value observed in our study ($10.79 \mu\text{g L}^{-1}$) slightly exceeding the upper limit of the Bavarian range. Moreover, in Germany, phenol concentrations range from 0.97 to $91.8 \mu\text{g L}^{-1}$, indicating a wide variability in contamination levels, with some samples showing significantly high contamination. In contrast, phenol concentrations are significantly lower in the current study, ranging from 0.08 to $4.4 \mu\text{g L}^{-1}$, which suggests lower contamination levels than those observed in Bavaria. The highest concentrations of o,m,p-cresols, in our study, reach a level of $12.0 \mu\text{g L}^{-1}$, which is slightly higher than the maximum level observed in Bavaria [19]. This comparison suggests that contamination levels at our sites are generally lower than those observed in Bavaria in 1990, except for 3-M-4-NPh, which shows comparable levels of contamination.

3.2. Acidic Compounds

3.2.1. MCA and DCA Concentrations

Thirteen DCA and twenty-five MCA are detected in the collected fog samples over the sampling period. The total concentration of the analyzed DCA varies from 3.4 to $101.4 \mu\text{g L}^{-1}$, whereas that of MCA varies from 14.3 to $180.6 \mu\text{g L}^{-1}$. The individual ratio of MCA to DCA is always higher than 1 (up to 5.8), except for three fog samples whose ratios vary from 0.5 to 0.8. For instance, MCA levels vary between 14.1 and $180.1 \mu\text{g L}^{-1}$, whereas those of DCA vary between 3.2 and $101.6 \mu\text{g L}^{-1}$. The highest levels are observed at Strasbourg (median of $48.4 \mu\text{g L}^{-1}$) followed by Cronenbourg (median of $42.3 \mu\text{g L}^{-1}$), Geispolsheim (median of $41.4 \mu\text{g L}^{-1}$), and Erstein (median of $34.3 \mu\text{g L}^{-1}$). Those levels are the highest among all previously analyzed organics due to their highest hygroscopicity. MCA (saturated and unsaturated) have been detected at all sampling sites with DF of 100%, except for C7 whose DF is 90%, whereas DCA is detected with DF higher than 80%. Lower molecular weight (C7–C18) is found to be more concentrated than high molecular weight (C19–C30). This might be explained by the higher water solubility of short-chain acids compared to long-chain organic acids, and the higher oxidative degradation of long-chain organic acids to short-chain organic acids. This is consistent with previous studies performed on clouds and rainwaters [45,84,105].

Figure 5 illustrates boxplots showing the levels of fog sample contamination with DCA and MCA. The boxplot reveals that the most abundant DCAs detected in the region are succinic acid, suberic acid, sebacic acid, and oxalic acid whose levels vary in the range of 0.3 – $29.5 \mu\text{g L}^{-1}$ (median of $2.5 \mu\text{g L}^{-1}$), 0.2 – $16.2 \mu\text{g L}^{-1}$ (median of $1.7 \mu\text{g L}^{-1}$), 0.3 – $11.1 \mu\text{g L}^{-1}$ (median of $1.7 \mu\text{g L}^{-1}$), and n.d.– $7.5 \mu\text{g L}^{-1}$ (median of $1.5 \mu\text{g L}^{-1}$). Oxalic acid consistently exhibits the highest concentrations across all sites, but the concentration levels vary significantly. For example, at certain sites, oxalic acid concentrations can be up to five times higher than at others. The variability across sites suggests that atmospheric

processes, like photochemical reactions, might be more intense at some locations, possibly due to differences in sunlight exposure or the presence of more important pollutant sources. Succinic acid shows moderate to high concentrations across all sites, with some sites having noticeably higher levels. The variability of succinic acid is more pronounced at the four locations, which suggests that these sites may have greater emissions of precursor compounds, such as VOCs, which oxidize into succinic acid. The concentration of suberic acid varies notably between sites, with some showing higher levels and wider variability. This could indicate that the sources of suberic acid—such as vehicle emissions and industrial processes—are more concentrated in certain areas. Sebacic acid is present at lower concentrations but still exhibits site-specific variability, which is likely influenced by different sources.

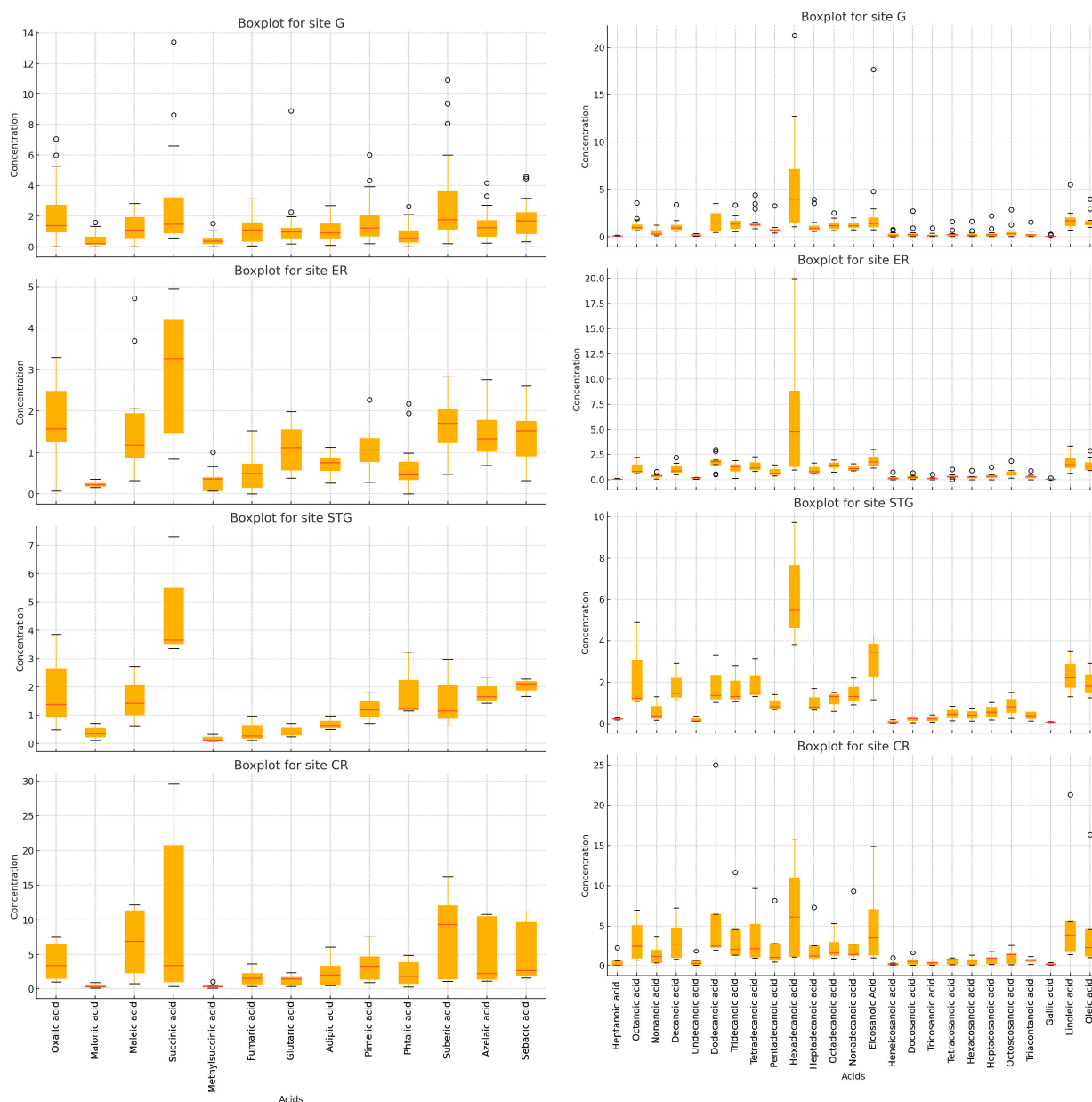


Figure 5. Boxplots of DCA (left hand side) and MCA (right hand side) across the four sampling sites.

The three MCAs that occupy the top levels are hexadecanoic acid (C16), dodecanoic acid (C12), and eicosanoic acid (C20), whose levels vary in the range of 0.9–21.3 $\mu\text{g L}^{-1}$ (median of 4.7 $\mu\text{g L}^{-1}$), 0.5–25.2 $\mu\text{g L}^{-1}$ (median of 1.9 $\mu\text{g L}^{-1}$), and 0.7–17.7 $\mu\text{g L}^{-1}$ (median

of $1.6 \mu\text{g L}^{-1}$). C16 is significantly the highest in concentration and is mainly derived from the intensive agricultural activities (which is a major source in the region), the combustion of biofuels and fossil fuels (vehicular exhaust and industries), and food processing and waste (i.e., food production or cooking activities). It exhibits the highest concentrations, with noticeable variability at some locations (such as Strasbourg and Cronenbourg). The wide range of values is indicative of some fluctuating conditions that impact its emissions across the different samples collected at a specific site over the sampling period. The timing of agricultural activities (use of fertilizers, harvesting, etc.), can vary from one year to another depending on the meteorological conditions in addition to the variation in industrial and traffic emissions (intensity, fuel usage, etc.). Thus, the daily variations in human activity between day and night or between weekdays and weekends are mainly responsible for the variation of its levels.

3.2.2. Atmospheric Sources in Fogwater

The secondary production of organic acids in the gas phase and their subsequent dissolution into the aqueous phase (fogwater droplet) is one of the main sources of MCA. They can also result from the dissolution of the soluble part of organic particles like oxalic, succinic, malonic, and maleic acids. Secondary emissions might include the photochemical transformation of precursors in the gaseous, aqueous, and particulate phases [106]. Metals such as manganese, iron, nickel, and copper show a good correlation (between 0.5 and 0.7, for $p < 0.05$) with organic acids [96]. Those metals can produce reactive species (such as OH radicals) that oxidize organic acids leading to the formation of SOAs. In fact, atmospheric hydrogen peroxide can break down on a solid catalyst producing OH radicals, which are capable of oxidizing organics at very mild conditions [107]. Furthermore, organic acids are primarily derived from direct human-made activities, particularly released from the industrial, transportation (motor exhaust emissions), and agricultural (biomass accumulation and burning) sectors [77]. Phthalic acid is an indicator of anthropogenic activities [108] and is detected in the range of $0.5\text{--}1.1 \mu\text{g L}^{-1}$. Also, bacterial metabolism generates a variety of short-chain carboxylic acids, thus another source may be the decomposition of the organic matter (e.g., soil and manure). MCA is found to be highly correlated with DCA (0.82 for $p < 0.001$) indicating similar sources for both. Moreover, the atmospheric malonic to succinic (M/S) ratio is helpful as source determination. A low ratio of M/S (between 0.3 and 0.5) indicates vehicular transport, while a higher ratio indicates secondary processes [109]. In our study, low ratios are observed in most fog samples, except in one sample (ratio of 1.7) indicating vehicular emissions. Pearson's analysis shows that there is no correlation between the organic acids and major inorganic acids (particularly sulfate and nitrate, which have been previously analyzed) suggesting that their formation is more affected by secondary emissions rather than anthropogenic activities [95]. Strong significant correlations are found among most of the analyzed organic acids (between 0.61 and 0.99, for $p < 0.001$) indicating good similarities in their emission, local sources, and environmental process (see Figure 6). Thus, organic acids have a double source emission in the investigated region, either from vehicular transport or through SOA formation.

3.2.3. Comparison of Acids with a Previous Study

Individual organic acid concentrations observed in our study are compared to another study that has been carried out at Hokkaido in Japan during 2020 and 2021 (see Table 1). In that study, fog sampling is performed at a mountain site isolated from the major agriculture and pasture areas. Mean concentrations of organic acids are comparable to those reported at Hokkaido (slightly lower for most compounds), except for oxalic, malonic, and succinic acids, whose levels are much lower than those observed at Hokkaido. In our study, their mean concentrations are, respectively, 1.5 , 0.2 , and 2.4 ng L^{-1} compared to 467.0 ng L^{-1} (May) and 89.0 ng L^{-1} (July), 59.0 ng L^{-1} (May) and 7.2 ng L^{-1} (July), and 156.0 ng L^{-1} (May) and 14.0 ng L^{-1} (July). The most significant reason can be related to differences in atmospheric oxidants. The lower temperature at the different sites in

Strasbourg metropolitan during winter time and reduced photochemical activity lead to lower atmospheric oxidants like ozone and radicals (OH and NO₃), which are essential to break down VOCs into smaller oxidized compounds, including organic acids. In contrast, the higher temperature during the late spring/early summer months in the mountainous environment in Hokkaido increases the photochemical activity driven by solar radiation and biogenic VOC emissions, facilitating the formation of organic acids. Therefore, the presence of oxidants enhances the organic acid formation because of the more important aqueous phase oxidation. In summary, while both studies identified similar organic acids, the variability in concentrations suggests that environmental factors such as climate, seasonality, and possible local sources play a critical role in the distribution and concentration levels of organic acids [98].

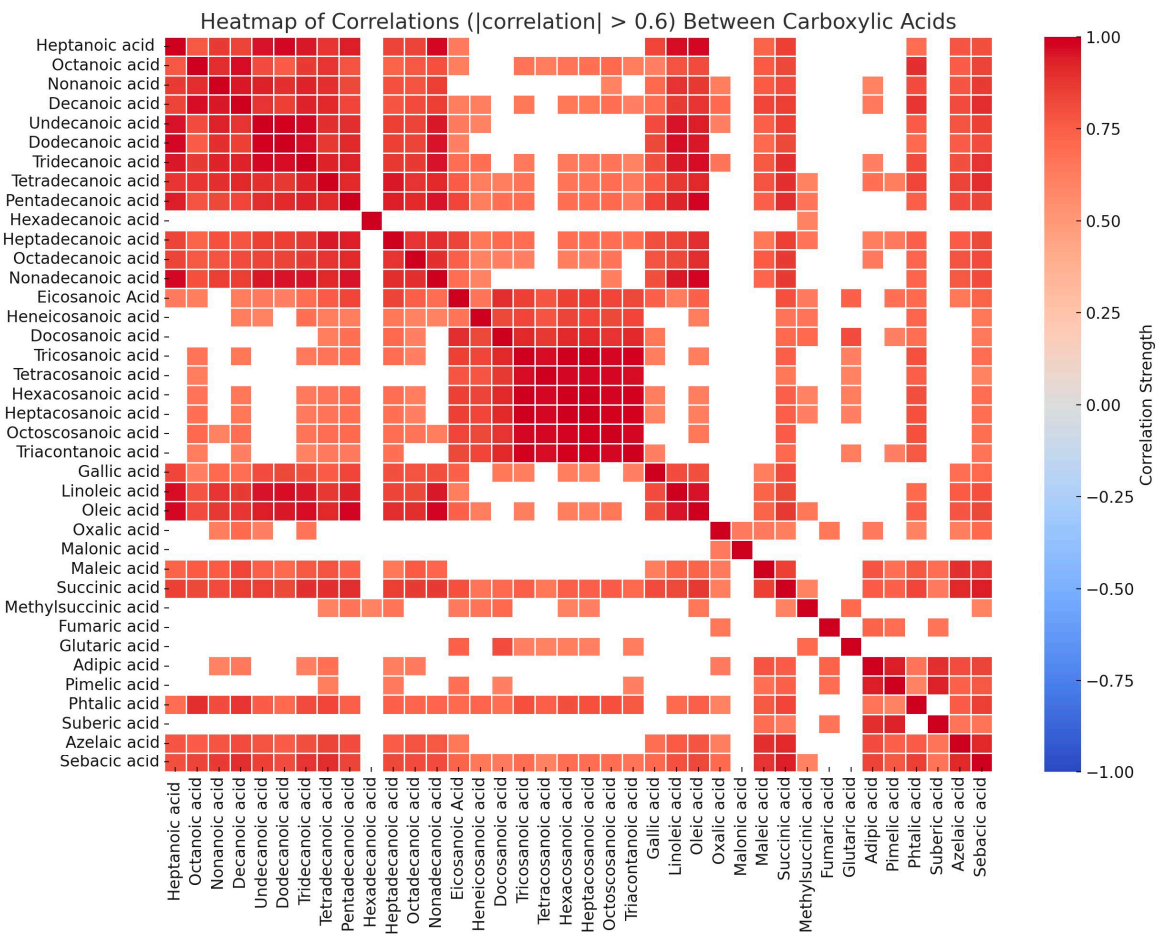


Figure 6. Heatmap of correlations (|correlation| > 0.6) between the different organic acids.

Table 1. Comparison of acid concentrations (ng L^{−1}) with those observed in mountain site of Hokkaido.

	This Study (October–December)	[98] (May)	[98] (July)
Heptanoic acid	0.07 (n.d.–2.3)	1.0 (0.4–2.3)	1.6 (n.d.–3.8)
Octanoic acid	1.0 (0.6–6.9)	0.4 (n.d.–0.8)	0.3 (n.d.–0.7)
Nonanoic acid	0.3 (0.09–3.6)	n.d.	1.2 (n.d.–8.6)
Decanoic acid	0.9 (0.5–7.2)	1.3 (0.02–2.4)	0.3 (n.d.–1.6)
Oxalic acid	1.5 (n.d.–7.4)	467.0 (218.0–754.0)	89.0 (27.0–335.0)
Malonic acid	0.2 (n.d.–1.5)	59.0 (28.0–83.0)	7.2 (n.d.–39.0)
Maleic acid	1.1 (n.d.–12.1)	9.9 (1.3–22.0)	2.1 (n.d.–8.0)
Succinic acid	2.4 (0.3–29.5)	156.0 (n.d.–374)	14.0 (1.0–48.0)
Methyl succinic acid	0.3 (n.d.–1.5)	3.6 (n.d.–14.0)	3.7 (0.3–12.2)

Table 1. Cont.

	This Study (October–December)	[98] (May)	[98] (July)
Fumaric acid	0.7 (n.d.–3.6)	27.0 (n.d.–64.0)	2.0 (0.8–3.6)
Glutaric acid	0.9 (0.1–8.8)	n.d.	5.0 (0.2–11.1)
Adipic acid	0.7 (0.07–6.1)	20.0 (5.9–42.0)	3.3 (1.2–7.5)
Pimelic acid	1.2 (0.1–7.7)	n.d.	1.1 (n.d.–2.0)
Phthalic acid	0.5 (n.d.–4.9)	8.7 (n.d.–16.0)	7.0 (0.2–11.0)
Suberic acid	1.7 (0.2–16.2)	n.d.	1.7 (n.d.–4.7)
Azelaic acid	1.3 (0.2–10.8)	0.8 (n.d.–3.1)	2.6 (0.9–6.2)
Sebacic acid	1.6 (0.3–11.2)	1.3 (n.d.–5.3)	2.6 (0.9–6.2)

n.d.—not detected/below the detection limit

Supplementary Materials: The following supporting information can be downloaded at: <https://www.mdpi.com/article/10.3390/atmos15101240/s1>, Table S1. Samples collected from the Alsace region at the four sampling sites during all years; Table S2. Validation parameters for carboxylic acids; Table S3. Validation parameters for dicarboxylic acids; Table S4. Validation parameters for phenols; Figure S1. Map of the studied region (Google Earth).

Author Contributions: Conceptualization, D.K., M.M., Y.J. and O.D.; methodology and experimentation: D.K.; validation, D.K., M.M., Y.J. and O.D.; data curation, D.K.; writing—original draft preparation, D.K.; writing—review and editing, D.K., M.M., Y.J. and O.D.; supervision, M.M., Y.J. and O.D.; project administration, M.M. All authors have read and agreed to the published version of the manuscript.

Funding: This research received no external funding.

Institutional Review Board Statement: Not applicable.

Informed Consent Statement: Not applicable.

Data Availability Statement: Data in this study are available upon request from the first author due to technical issues while recovering them from the software.

Conflicts of Interest: The authors declare no conflicts of interest.

Abbreviations

Phenols	Abb.	Phenols	Abb.	Acids	Abb.
Meta-cresol	m-cresol	2,4-dinitrophenol	2,4-DNPh	Heptanoic acid	C7
Ortho-cresol	o-cresol	2,5-dinitrophenol	2,5-DNPh	Octanoic acid	C8
Para-cresol	p-cresol	2,6-dinitrophenol	2,6-DNPh	Nonanoic acid	C9
2-chlorophenol	3-CPh	3,4-dinitrophenol	3,4-DNPh	Decanoic acid	C10
3-chlorophenol	3-CPh	2-nitrophenol	2-NPh	Undecanoic acid	C11
4-chlorophenol	3-CPh	3-nitrophenol	3-NPh	Dodecanoic acid	C12
3,5-dichlorophenol	3,5-DCPh	4-nitrophenol	4-NPh	Tridecanoic acid	C13
2,5-dichlorophenol	2,5-DCPh	2-bromophenol	2-BPh	Tetradecanoic acid	C14
2,4-dichlorophenol	2,4-DCPh	4-bromophenol	4-BPh	Hexadecanoic acid	C16
2,3-dichlorophenol	2,3-DCPh	2,6-dibromophenol	2,6-DBPh	Heptadecanoic acid	C17
2,3,5-trichlorophenol	2,3,5-TCHPh	2-aminophenol	2-APh	Octadecanoic acid	C18
2,4,5-trichlorophenol	2,4,5-TCHPh	4-aminophenol	4-APh	Nonadecanoic acid	C19
3,4,5-trichlorophenol	3,4,5-TCHPh	2,4-dinitrophenol	2,4-DNPh	Eicosanoic Acid	C20
2,3,6-trichlorophenol	2,3,6-TCHPh	2,5-dinitrophenol	2,5-DNPh	Heneicosanoic acid	C21
2,3,4-trichlorophenol	2,3,4-TCHPh	2,6-dinitrophenol	2,6-DNPh	Docosanoic acid	C22
Pentachlorophenol	PCPh	3,4-dinitrophenol	3,4-DNPh	Tricosanoic acid	C23
3-methyl-2-nitrophenol	3-M-2-NPh	2-nitrophenol	2-NPh	Tetracosanoic acid	C24
3-methyl-4-nitrophenol	3-M-4-NPh	3-nitrophenol	3-NPh	Hexacosanoic acid	C26
4-methyl-2-nitrophenol	4-M-2-NPh	4-nitrophenol	4-NPh	Heptacosanoic acid	C27
5-methyl-2-nitrophenol	5-M-2-NPh	2-bromophenol	2-BPh	Octocosanoic acid	C28
6-methyl-2-nitrophenol	6-M-2-NPh	3-bromophenol	3-BPh	Triacontanoic acid	C30

References

1. Facchini, M.C.; Decesari, S.; Mircea, M.; Fuzzi, S.; Loglio, G. Surface tension of atmospheric wet aerosol and cloud/fog droplets in relation to their organic carbon content and chemical composition. *Atmos. Environ.* **2000**, *34*, 4853–4857. [\[CrossRef\]](#)
2. Allen, S.K.; Allen, C.W. Phenol concentrations in air and rain water samples collected near a wood preserving facility. *Bull. Environ. Contam. Toxicol.* **1997**, *59*, 702–707. [\[CrossRef\]](#)
3. Shea, P.J.; Weber, J.B.; Overcash, M.R. Biological activities of 2, 4-dinitrophenol in plant-soil systems. In *Residue Reviews: Residues of Pesticides and Other Contaminants in the Total Environment*; Springer: New York, NY, USA, 1983; pp. 1–41. [\[CrossRef\]](#)
4. Shafer, W.E.; Schönherr, J. Accumulation and transport of phenol, 2-nitrophenol, and 4-nitrophenol in plant cuticles. *Ecotoxicol. Environ. Saf.* **1985**, *10*, 239–252. [\[CrossRef\]](#)
5. Rippen, G.; Zietz, E.; Frank, R.; Knacker, T.; Klöpffer, W. Do airborne nitrophenols contribute to forest decline? *Environ. Technol.* **1987**, *8*, 475–482. [\[CrossRef\]](#)
6. Trautner, F.; Reischl, A.; Hutzinger, O. Nitrierte Phenole in Nebelwasser: Beitrag zur Waldschadensforschung. *Umweltwissenschaften Schadst. Forsch.* **1989**, *1*, 10–11. [\[CrossRef\]](#)
7. Leuenberger, C.; Czuczwa, J.; Tremp, J.; Giger, W. Nitrated phenols in rain: Atmospheric occurrence of phytotoxic pollutants. *Chemosphere* **1988**, *17*, 511–515. [\[CrossRef\]](#)
8. Environmental Protection Agency (EPA), 2014, Priority Pollutant List. Available online: <https://www.epa.gov/sites/default/files/2015-09/documents/priority-pollutant-list-epa.pdf> (accessed on 15 December 2014).
9. Schüssler, W.; Nitschke, L. Nitrophenols in precipitation. *Chemosphere* **2001**, *42*, 277–283. [\[CrossRef\]](#)
10. Kawamura, K.; Kaplan, I.R. Organic compounds in the rainwater of Los Angeles. *Environ. Sci. Technol.* **1983**, *17*, 497–501. [\[CrossRef\]](#)
11. Leuenberger, C.; Ligocki, M.P.; Pankow, J.F. Trace organic compounds in rain. 4. Identities, concentrations, and scavenging mechanisms for phenols in urban air and rain. *Environ. Sci. Technol.* **1985**, *19*, 1053–1058. [\[CrossRef\]](#)
12. Cecinato, A.; Di Palo, V.; Pomata, D.; Scianò, M.C.T.; Possanzini, M. Measurement of phase-distributed nitrophenols in Rome ambient air. *Chemosphere* **2005**, *59*, 679–683. [\[CrossRef\]](#)
13. Morville, S.; Scheyer, A.; Mirabel, P.; Millet, M. Spatial and geographical variations of urban, suburban and rural atmospheric concentrations of phenols and nitrophenols. *Environ. Sci. Pollut. Res.* **2006**, *13*, 83–89. [\[CrossRef\]](#)
14. Bishop, E.J.; Mitra, S. Measurement of nitrophenols in air samples by impinger sampling and supported liquid membrane micro-extraction. *Anal. Chim. Acta* **2007**, *583*, 10–14. [\[CrossRef\]](#)
15. Delhomme, O.; Morville, S.; Millet, M. Seasonal and diurnal variations of atmospheric concentrations of phenols and nitrophenols measured in the Strasbourg area, France. *Atmos. Pollut. Res.* **2010**, *1*, 16–22. [\[CrossRef\]](#)
16. Lüttke, J.; Levsen, K.; Acker, K.; Wieprecht, W.; Möller, D. Phenols and nitrated phenols in clouds at Mount Brocken. *Int. J. Environ. Anal. Chem.* **1999**, *74*, 69–89. [\[CrossRef\]](#)
17. Alber, M.; Böhm, H.B.; Brodesser, J.; Schöler, H.F.; Feltes, J.; Levsen, K. Determination of nitrophenols in rain and snow. *Anal. Chem.* **1989**, *334*, 540–545. [\[CrossRef\]](#)
18. Nojima, K.; Kawaguchi, A.; Ohya, T.; Kanno, S.; Hirobe, M. Studies on photochemical reaction of air pollutants. X. Identification of nitrophenols in suspended particulates. *Chem. Pharm. Bull.* **1983**, *31*, 1047–1051. [\[CrossRef\]](#)
19. Richartz, H.; Reischl, A.; Trautner, F.; Hutzinger, O. Nitrated phenols in fog. *Atmos. Environ. Part A Gen. Top.* **1990**, *24*, 3067–3071. [\[CrossRef\]](#)
20. Schwarzenbach, R.P.; Stierli, R.; Folsom, B.R.; Zeyer, J. Compound properties relevant for assessing the environmental partitioning of nitrophenols. *Environ. Sci. Technol.* **1988**, *22*, 83–92. [\[CrossRef\]](#)
21. Vanni, A.; Pellegrino, V.; Gamberini, R.; Calabria, A. An evidence for nitrophenols contamination in Antarctic fresh-water and snow. Simultaneous determination of nitrophenols and nitroarenes at ng/L levels. *Int. J. Environ. Anal. Chem.* **2001**, *79*, 349–365. [\[CrossRef\]](#)
22. Harrison, M.A.; Barra, S.; Borghesi, D.; Vione, D.; Arsene, C.; Olariu, R.I. Nitrated phenols in the atmosphere: A review. *Atmos. Environ.* **2005**, *39*, 231–248. [\[CrossRef\]](#)
23. Lu, C.; Wang, X.; Dong, S.; Zhang, J.; Li, J.; Zhao, Y.; Liang, Y.; Xue, L.; Xie, H.; Zhang, Q.; et al. Emissions of fine particulate nitrated phenols from various on-road vehicles in China. *Environ. Res.* **2019**, *179*, 108709. [\[CrossRef\]](#)
24. Lu, C.; Wang, X.; Li, R.; Gu, R.; Zhang, Y.; Li, W.; Gao, R.; Chen, B.; Xue, L.; Wang, W. Emissions of fine particulate nitrated phenols from residential coal combustion in China. *Atmos. Environ.* **2019**, *203*, 10–17. [\[CrossRef\]](#)
25. Wang, Y.; Hu, M.; Wang, Y.; Zheng, J.; Shang, D.; Yang, Y.; Liu, Y.; Li, X.; Tang, R.; Zhu, W.; et al. The formation of nitro-aromatic compounds under high NO_x and anthropogenic VOC conditions in urban Beijing, China. *Atmos. Chem. Phys.* **2019**, *19*, 7649–7665. [\[CrossRef\]](#)
26. Tremp, J.; Mattrel, P.; Fingler, S.; Giger, W.J.W.A. Phenols and nitrophenols as tropospheric pollutants: Emissions from automobile exhausts and phase transfer in the atmosphere. *Water Air Soil Pollut.* **1993**, *68*, 113–123. [\[CrossRef\]](#)
27. Bolzacchini, E.; Perrone, M.G.; Gianelle, V.; Rindone, B.; Avella, F.; Faedo, D.; Ierardi, P.; Astorga, C.; Hjorth, J. Nitrophenols in Milan atmosphere and urban particulate. In Proceedings of the 8th Symposium of the Environmental Chemistry Division, Italian Chemical Society, Siena, Italy, 8–11 June 2004.
28. Furuta, C.; Suzuki, A.K.; Watanabe, G.; Li, C.; Taneda, S.; Taya, K. Nitrophenols isolated from diesel exhaust particles promote the growth of MCF-7 breast adenocarcinoma cells. *Toxicol. Appl. Pharmacol.* **2008**, *230*, 320–326. [\[CrossRef\]](#)

29. Tompkins, C.J.; Michaels, A.S.; Peretti, S.W. Removal of p-nitrophenol from aqueous solution by membrane-supported solvent extraction. *J. Membr. Sci.* **1992**, *75*, 277–292. [\[CrossRef\]](#)
30. Rodriguez, I.; Llompарт, M.P.; Cela, R. Solid-phase extraction of phenols. *J. Chromatogr. A* **2000**, *885*, 291–304. [\[CrossRef\]](#)
31. Schlett, C.; Pfeifer, P. Bestimmung substituierter Phenole unterhalb des Geruchsschwellenwertes. *Vom Wasser* **1992**, *79*, 65–74.
32. Bejan, I.G.; Olariu, R.-I.; Wiesen, P. Secondary Organic Aerosol Formation from Nitrophenols Photolysis under Atmospheric Conditions. *Atmosphere* **2020**, *11*, 1346. [\[CrossRef\]](#)
33. Nojima, K.; Fukaya, K.; Fukui, S.; Kanno, S. Studies on photochemistry of aromatic hydrocarbons II: The formation of nitrophenols and nitrobenzene by the photochemical reaction of benzene in the presence of nitrogen monoxide. *Chemosphere* **1975**, *4*, 77–82. [\[CrossRef\]](#)
34. Nojima, K.; Fukaya, K.; Fukui, S.; Kanno, S.; Nishiyama, S.; Wada, Y. Studies on photochemistry of aromatic hydrocarbons III: Formation of nitrophenols by the photochemical reaction of toluene in the presence of nitrogen monoxide and nitrophenols in rain. *Chemosphere* **1976**, *5*, 25–30. [\[CrossRef\]](#)
35. Nojima, K.; Kanno, S. Studies on photochemistry of aromatic hydrocarbons. IV. Mechanism of formation of nitrophenols by the photochemical reaction of benzene and toluene with nitrogen oxides in air. *Chemosphere* **1977**, *6*, 371–376. [\[CrossRef\]](#)
36. Atkinson, R.; Carter, W.P.; Darnall, K.R.; Winer, A.M.; Pitts, J.N., Jr. A smog chamber and modeling study of the gas phase NO_x-air photooxidation of toluene and the cresols. *Int. J. Chem. Kinet.* **1980**, *12*, 779–836. [\[CrossRef\]](#)
37. Grosjean, D. Atmospheric reactions of ortho cresol: Gas phase and aerosol products. *Atmos. Environ.* **1984**, *18*, 1641–1652. [\[CrossRef\]](#)
38. Leone, J.A.; Seinfeld, J.H. Comparative analysis of chemical reaction mechanisms for photochemical smog. *Atmos. Environ.* **1985**, *19*, 437–464. [\[CrossRef\]](#)
39. Ng, N.L.; Kwan, A.J.; Surratt, J.D.; Chan, A.W.H.; Chhabra, P.S.; Sorooshian, A.; Pye, H.O.T.; Crounse, J.D.; Wennberg, P.O.; Flagan, R.C.; et al. Secondary organic aerosol (SOA) formation from reaction of isoprene with nitrate radicals (NO₃). *Atmos. Chem. Phys.* **2008**, *8*, 4117–4140. [\[CrossRef\]](#)
40. Atkinson, R.; Aschmann, S.M.; Arey, J. Reactions of hydroxyl and nitrogen trioxide radicals with phenol, cresols, and 2-nitrophenol at 296 ± 2 K. *Environ. Sci. Technol.* **1992**, *26*, 1397–1403. [\[CrossRef\]](#)
41. Bolzacchini, E.; Bruschi, M.; Hjorth, J.; Meinardi, S.; Orlandi, M.; Rindone, B.; Rosenbohm, E. Gas-phase reaction of phenol with NO₃. *Environ. Sci. Technol.* **2001**, *35*, 1791–1797. [\[CrossRef\]](#)
42. Cheng, X.; Chen, Q.; Li, Y.; Huang, G.; Liu, Y.; Lu, S.; Zheng, Y.; Qiu, W.; Lu, K.; Qiu, X.; et al. Secondary production of gaseous nitrated phenols in polluted urban environments. *Environ. Sci. Technol.* **2021**, *55*, 4410–4419. [\[CrossRef\]](#)
43. Bejan, I.; Abd El Aal, Y.; Barnes, I.; Benter, T.; Bohn, B.; Wiesen, P.; Kleffmann, J. The photolysis of ortho-nitrophenols: A new gas phase source of HONO. *Phys. Chem. Chem. Phys.* **2006**, *8*, 2028–2035. [\[CrossRef\]](#)
44. Schwantes, R.H.; Schilling, K.A.; McVay, R.C.; Lignell, H.; Coggon, M.M.; Zhang, X.; Wennberg, P.O.; Seinfeld, J.H. Formation of highly oxygenated low-volatility products from cresol oxidation. *Atmos. Chem. Phys.* **2017**, *17*, 3453–3474. [\[CrossRef\]](#)
45. Chebbi, A.; Carlier, P. Carboxylic acids in the troposphere, occurrence, sources, and sinks: A review. *Atmos. Environ.* **1996**, *30*, 4233–4249. [\[CrossRef\]](#)
46. Alier, M.; Osto, M.D.; Lin, Y.H.; Surratt, J.D.; Tauler, R.; Grimalt, J.O.; van Drooge, B.L. On the origin of water-soluble organic tracer compounds in fine aerosols in two cities: The case of Los Angeles and Barcelona. *Environ. Sci. Pollut. Res.* **2014**, *21*, 11649–11660. [\[CrossRef\]](#)
47. Li, X.D.; Yang, Z.; Fu, P.; Yu, J.; Lang, Y.C.; Liu, D.; Ono, K.; Kawamura, K. High abundances of dicarboxylic acids, oxocarboxylic acids and α-dicarbonyls in fine aerosols (PM_{2.5}) in Chengdu, China during wintertime haze pollution. *Environ. Sci. Pollut. Res.* **2015**, *22*, 12902–12918. [\[CrossRef\]](#)
48. Keene, W.C.; Galloway, J.N. The biogeochemical cycling of formic and acetic acids through the troposphere: An overview of current understanding. *Tellus B Chem. Phys. Meteorol.* **1988**, *40*, 322–334. [\[CrossRef\]](#)
49. Khare, P.; Kumar, N.; Kumari, K.M.; Srivastava, S.S. Atmospheric formic and acetic acids: An overview. *Rev. Geophys.* **1999**, *37*, 227–248. [\[CrossRef\]](#)
50. Sun, J.; Ariya, P.A. Atmospheric organic and bio-aerosols as cloud condensation nuclei (CCN): A review. *Atmos. Environ.* **2006**, *40*, 795–820. [\[CrossRef\]](#)
51. Bastidas, D.M.; La Iglesia, V.M. Organic acid vapours and their effect on corrosion of copper: A review. *Corros. Eng. Sci. Technol.* **2007**, *42*, 272–280. [\[CrossRef\]](#)
52. Nolte, C.G.; Fraser, M.P.; Cass, G.R. Gas phase C₂–C₁₀ organic acids concentrations in the Los Angeles atmosphere. *Environ. Sci. Technol.* **1999**, *33*, 540–545. [\[CrossRef\]](#)
53. Kawamura, K.; Ng, L.L.; Kaplan, I.R. Determination of organic acids (C₁–C₁₀) in the atmosphere, motor exhausts, and engine oils. *Environ. Sci. Technol.* **1985**, *19*, 1082–1086. [\[CrossRef\]](#)
54. Satsumabayashi, H.; Kurita, H.; Yokouchi, Y.; Ueda, H. Mono- and di-carboxylic acids under long-range transport of air pollution in central Japan. *Tellus B Chem. Phys. Meteorol.* **1989**, *41*, 219–229. [\[CrossRef\]](#)
55. Pye, H.O.; Nenes, A.; Alexander, B.; Ault, A.P.; Barth, M.C.; Clegg, S.L.; Collett, J.L., Jr.; Fahey, K.M.; Hennigan, C.J.; Herrmann, H.; et al. The acidity of atmospheric particles and clouds. *Atmos. Chem. Phys.* **2020**, *20*, 4809–4888. [\[CrossRef\]](#)

56. Mochizuki, T.; Kawamura, K.; Nakamura, S.; Kanaya, Y.; Wang, Z. Enhanced levels of atmospheric low-molecular weight monocarboxylic acids in gas and particulates over Mt. Tai, North China, during field burning of agricultural wastes. *Atmos. Environ.* **2017**, *171*, 237–247. [\[CrossRef\]](#)
57. Andreae, M.O.; Talbot, R.W.; Andreae, T.W.; Harriss, R.C. Formic and acetic acid over the central Amazon region, Brazil: 1. Dry season. *J. Geophys. Res. Atmos.* **1988**, *93*, 1616–1624. [\[CrossRef\]](#)
58. Mochizuki, T.; Kawamura, K.; Aoki, K.; Sugimoto, N. Long-range atmospheric transport of volatile monocarboxylic acids with Asian dust over a high mountain snow site, central Japan. *Atmos. Chem. Phys.* **2016**, *16*, 14621–14633. [\[CrossRef\]](#)
59. Veres, P.R.; Roberts, J.M.; Cochran, A.K.; Gilman, J.B.; Kuster, W.C.; Holloway, J.S.; Graus, M.; Flynn, J.; Lefer, B.; Warneke, C.; et al. Evidence of rapid production of organic acids in an urban air mass. *Geophys. Res. Lett.* **2011**, *38*. [\[CrossRef\]](#)
60. Zemankova, K.; Brechler, J. Emissions of biogenic VOC from forest ecosystems in central Europe: Estimation and comparison with anthropogenic emission inventory. *Environ. Pollut.* **2010**, *158*, 462–469. [\[CrossRef\]](#)
61. Cheung, K.L.; Ntziachristos, L.; Tzamkiozis, T.; Schauer, J.J.; Samaras, Z.; Moore, K.F.; Sioutas, C. Emissions of particulate trace elements, metals and organic species from gasoline, diesel, and biodiesel passenger vehicles and their relation to oxidative potential. *Aerosol Sci. Technol.* **2010**, *44*, 500–513. [\[CrossRef\]](#)
62. Gomez, S.L.; Carrico, C.M.; Allen, C.; Lam, J.; Dabli, S.; Sullivan, A.P.; Aiken, A.C.; Rahn, T.; Romonosky, D.; Chylek, P.; et al. Southwestern US biomass burning smoke hygroscopicity: The role of plant phenology, chemical composition, and combustion properties. *J. Geophys. Res. Atmos.* **2018**, *123*, 5416–5432. [\[CrossRef\]](#)
63. Grosjean, D. Organic acids in southern California air: Ambient concentrations, mobile source emissions, in situ formation and removal processes. *Environ. Sci. Technol.* **1989**, *23*, 1506–1514. [\[CrossRef\]](#)
64. Talbot, R.W.; Beecher, K.M.; Harriss, R.C.; Cofer III, W.R. Atmospheric geochemistry of formic and acetic acids at a mid-latitude temperate site. *J. Geophys. Res. Atmos.* **1988**, *93*, 1638–1652. [\[CrossRef\]](#)
65. Talbot, R.W.; Andreae, M.O.; Berresheim, H.; Jacob, D.J.; Beecher, K.M. Sources and sinks of formic, acetic, and pyruvic acids over central Amazonia: 2. Wet season. *J. Geophys. Res. Atmos.* **1990**, *95*, 16799–16811. [\[CrossRef\]](#)
66. Keene, W.C.; Galloway, J.N. Considerations regarding sources for formic and acetic acids in the troposphere. *J. Geophys. Res. Atmos.* **1986**, *91*, 14466–14474. [\[CrossRef\]](#)
67. Khare, P.; Satsangi, G.S.; Kumar, N.; Kumari, K.M.; Srivastava, S.S. Surface measurements of formaldehyde and formic and acetic acids at a subtropical semiarid site in India. *J. Geophys. Res. Atmos.* **1997**, *102*, 18997–19005. [\[CrossRef\]](#)
68. Calvert, J.G.; Madronich, S. Theoretical study of the initial products of the atmospheric oxidation of hydrocarbons. *J. Geophys. Res. Atmos.* **1987**, *92*, 2211–2220. [\[CrossRef\]](#)
69. Duce, R.A.; Mohnen, V.A.; Zimmerman, P.R.; Grosjean, D.; Cautreels, W.; Chatfield, R.; Jaenicke, R.; Ogren, J.A.; Pellizzari, E.D.; Wallace, G.T. Organic material in the global troposphere. *Rev. Geophys.* **1983**, *21*, 921–952. [\[CrossRef\]](#)
70. Madronich, S.; Calvert, J.G. Permutation reactions of organic peroxy radicals in the troposphere. *J. Geophys. Res. Atmos.* **1990**, *95*, 5697–5715. [\[CrossRef\]](#)
71. Kawamura, K.; Imai, Y.; Barrie, L.A. Photochemical production and loss of organic acids in high Arctic aerosols during long-range transport and polar sunrise ozone depletion events. *Atmos. Environ.* **2005**, *39*, 599–614. [\[CrossRef\]](#)
72. Orzechowska, G.E.; Paulson, S.E. Photochemical sources of organic acids. 1. Reaction of ozone with isoprene, propene, and 2-butenes under dry and humid conditions using SPME. *J. Phys. Chem. A* **2005**, *109*, 5358–5365. [\[CrossRef\]](#)
73. Mattila, J.M.; Brophy, P.; Kirkland, J.; Hall, S.; Ullmann, K.; Fischer, E.V.; Brown, S.; McDuffie, E.; Tevlin, A.; Farmer, D.K. Tropospheric sources and sinks of gas-phase acids in the Colorado Front Range. *Atmos. Chem. Phys.* **2018**, *18*, 12315–12327. [\[CrossRef\]](#)
74. Avery, G.B., Jr.; Willey, J.D.; Wilson, C.A. Formic and acetic acids in coastal North Carolina rainwater. *Environ. Sci. Technol.* **1991**, *25*, 1875–1880. [\[CrossRef\]](#)
75. Nolte, C.G.; Solomon, P.A.; Fall, T.; Salmon, L.G.; Cass, G.R. Seasonal and spatial characteristics of formic and acetic acids concentrations in the southern California atmosphere. *Environ. Sci. Technol.* **1997**, *31*, 2547–2553. [\[CrossRef\]](#)
76. Paulot, F.; Wunch, D.; Crounse, J.D.; Toon, G.C.; Millet, D.B.; DeCarlo, P.F.; Vigouroux, C.; Deutscher, N.M.; González Abad, G.; Notholt, J.; et al. Importance of secondary sources in the atmospheric budgets of formic and acetic acids. *Atmos. Chem. Phys.* **2011**, *11*, 1989–2013. [\[CrossRef\]](#)
77. Xie, Y.; Lu, H.; Yi, A.; Zhang, Z.; Zheng, N.; Fang, X.; Xiao, H. Characterization and source analysis of water-soluble ions in PM_{2.5} at a background site in Central China. *Atmos. Res.* **2020**, *239*, 104881. [\[CrossRef\]](#)
78. Legrand, M.; Preunkert, S.; Galy-Lacaux, C.; Lioussé, C.; Wagenbach, D. Atmospheric year-round records of dicarboxylic acids and sulfate at three French sites located between 630 and 4360 m elevation. *J. Geophys. Res. Atmos.* **2005**, *110*, D13302. [\[CrossRef\]](#)
79. Sellegri, K.; Laj, P.; Marinoni, A.; Dupuy, R.; Legrand, M.; Preunkert, S. Contribution of gaseous and particulate species to droplet solute composition at the Puy de Dôme, France. *Atmos. Chem. Phys.* **2003**, *3*, 1509–1522. [\[CrossRef\]](#)
80. Servant, J.; Kouadio, G.; Cros, B.; Delmas, R. Carboxylic monoacids in the air of Mayombe forest (Congo): Role of the forest as a source or sink. *J. Atmos. Chem.* **1991**, *12*, 367–380. [\[CrossRef\]](#)
81. Peña, R.M.; García, S.; Herrero, C.; Losada, M.; Vázquez, A.; Lucas, T. Organic acids and aldehydes in rainwater in a northwest region of Spain. *Atmos. Environ.* **2002**, *36*, 5277–5288. [\[CrossRef\]](#)
82. Puxbaum, H.; Rosenberg, C.; Gregori, M.; Lanzerstorfer, C.; Ober, E.; Winiwarter, W. Atmospheric concentrations of formic and acetic acid and related compounds in eastern and northern Austria. *Atmos. Environ.* **1988**, *22*, 2841–2850. [\[CrossRef\]](#)

83. Grosjean, D. Formic acid and acetic acid: Emissions, atmospheric formation and dry deposition at two southern California locations. *Atmos. Environ. Part A Gen. Top.* **1992**, *26*, 3279–3286. [\[CrossRef\]](#)
84. Helas, G.; Bingemer, H.; Andreae, M.O. Organic acids over equatorial Africa: Results from DECAFE 88. *J. Geophys. Res. Atmos.* **1992**, *97*, 6187–6193. [\[CrossRef\]](#)
85. Sakugawa, H.; Kaplan, I.R.; Shepard, L.S. Measurements of H₂O₂, aldehydes and organic acids in Los Angeles rainwater: Their sources and deposition rates. *Atmos. Environ. Part B Urban Atmos.* **1993**, *27*, 203–219. [\[CrossRef\]](#)
86. Khwaja, H.A. Atmospheric concentrations of carboxylic acids and related compounds at a semiurban site. *Atmos. Environ.* **1995**, *29*, 127–139. [\[CrossRef\]](#)
87. Souza, S.R.; Vasconcellos, P.C.; Carvalho, L.R. Low molecular weight carboxylic acids in an urban atmosphere: Winter measurements in Sao Paulo City, Brazil. *Atmos. Environ.* **1999**, *33*, 2563–2574. [\[CrossRef\]](#)
88. Bokwa, A.; Wypych, A.; Hajto, M.J. Impact of Natural and Anthropogenic Factors on Fog Frequency and Variability in Kraków, Poland in the Years 1966–2015. *Aerosol Air Qual. Res.* **2018**, *18*, 165–177. [\[CrossRef\]](#)
89. Helas, G.; Andreae, M.O.; Hartmann, W.R. Behavior of atmospheric formic and acetic acid in the presence of hydrometeors. *J. Atmos. Chem.* **1992**, *15*, 101–115. [\[CrossRef\]](#)
90. Millet, M. Etude de la Composition Chimique des Brouillards et Analyse des Pesticides dans les Phases Liquide, Gazeuse et Particulaire de L'atmosphère. Ph.D. Thesis, Université Louis Pasteur, Strasbourg, France, 1994; p. 204.
91. Millet, M.; Sanusi, A.; Wortham, H. Chemical composition of fogwater in an urban area: Strasbourg (France). *Environ. Pollut.* **1996**, *94*, 345–354. [\[CrossRef\]](#)
92. Millet, M.; Wortham, H.; Sanusi, A.; Mirabel, P. Low molecular weight organic acids in fogwater in an urban area: Strasbourg (France). *Sci. Total Environ.* **1997**, *206*, 57–65. [\[CrossRef\]](#)
93. Millet, M.; Wortham, H.; Sanusi, A.; Mirabel, P. Atmospheric contamination by pesticides: Determination in the liquid, gaseous and particulate phases. *Environ. Sci. Pollut. Res.* **1997**, *4*, 172–180. [\[CrossRef\]](#)
94. Herckes, P.; Wortham, H.; Mirabel, P.; Millet, M. Evolution of the fogwater composition in Strasbourg (France) from 1990 to 1999. *Atmos. Res.* **2002**, *64*, 53–62. [\[CrossRef\]](#)
95. Khoury, D.; Millet, M.; Jabali, Y.; Weissenberger, T.; Delhomme, O. Spatio-temporal evolution of fogwater chemistry in Alsace. *Air* **2024**, *2*, 229–246. [\[CrossRef\]](#)
96. Khoury, D.; Millet, M.; Jabali, Y.; Delhomme, O. Occurrence of Polycyclic Aromatic Hydrocarbons and Polychlorinated Biphenyls in Fogwater at Urban, Suburban, and Rural Sites in Northeast France between 2015 and 2021. *Atmosphere* **2024**, *15*, 291. [\[CrossRef\]](#)
97. Khoury, D.; Jabali, Y.; Delhomme, O.; Millet, M. Pesticide occurrence and distribution in fogwater collected at four sites at Strasbourg metropolitan between 2015 and 2021. *Environ. Pollut.* **2024**, *359*, 124564. [\[CrossRef\]](#)
98. Mochizuki, T.; Kawamura, K.; Yamaguchi, T.; Noguchi, I. Distributions and sources of water-soluble organic acids in fog water from mountain site (Lake Mashu) of Hokkaido, Japan. *Geochem. J.* **2020**, *54*, 315–326. [\[CrossRef\]](#)
99. Demoz, B.B.; Collett, J.L., Jr.; Daube, B.C., Jr. On the Caltech active strand cloudwater collectors. *Atmos. Res.* **1996**, *41*, 47–62. [\[CrossRef\]](#)
100. Daube, B.C., Jr.; Flagan, R.C.; Hoffmann, M.R. California Institute of Technology CalTech. Active Cloudwater Collector. U.S. Patent 4,697,462, 6 October 1987.
101. Khoury, D.; Millet, M.; Jabali, Y.; Delhomme, O. Analytical procedure for the concomitant analysis of 242 polar and non-polar organic compounds of different functional groups in fog water. *Microchem. J.* **2023**, *185*, 108235. [\[CrossRef\]](#)
102. Roumeliotis, P.; Liebal, W.; Unger, K.K. Determination of phenols from automobile exhaust by means of high-performance liquid chromatography (HPLC). *Int. J. Environ. Anal. Chem.* **1983**, *9*, 27–43. [\[CrossRef\]](#)
103. Rubio, M.A.; Guerrero, M.J.; Villena, G.; Lissi, E. Hydroperoxides in dew water in downtown Santiago, Chile. A comparison with gas-phase values. *Atmos. Environ.* **2006**, *40*, 6165–6172. [\[CrossRef\]](#)
104. Schummer, C.; Groff, C.; Al Chami, J.; Jaber, F.; Millet, M. Analysis of phenols and nitrophenols in rainwater collected simultaneously on an urban and rural site in east of France. *Sci. Total Environ.* **2009**, *407*, 5637–5643. [\[CrossRef\]](#)
105. Tanner, P.A.; Law, P.T. Organic acids in the atmosphere and bulk deposition of Hong Kong. *Water Air Soil Pollut.* **2003**, *142*, 279–297. [\[CrossRef\]](#)
106. Munger, J.W.; Jacob, D.J.; Waldman, J.M.; Hoffmann, M.R. Fogwater chemistry in an urban atmosphere. *J. Geophys. Res. Ocean.* **1983**, *88*, 5109–5121. [\[CrossRef\]](#)
107. Rey, A.; Bahamonde, A.; Casas, J.A.; Rodríguez, J.J. Selectivity of hydrogen peroxide decomposition towards hydroxyl radicals in catalytic wet peroxide oxidation (CWPO) over Fe/AC catalysts. *Water Sci. Technol.* **2010**, *61*, 2769–2778. [\[CrossRef\]](#)
108. Kawamura, K.; Kaplan, I.R. Motor exhaust emissions as a primary source for dicarboxylic acids in Los Angeles ambient air. *Environ. Sci. Technol.* **1987**, *21*, 105–110. [\[CrossRef\]](#)
109. Yao, X.; Fang, M.; Chan, C.K.; Ho, K.F.; Lee, S.C. Characterization of dicarboxylic acids in PM_{2.5} in Hong Kong. *Atmos. Environ.* **2004**, *38*, 963–970. [\[CrossRef\]](#)

Disclaimer/Publisher's Note: The statements, opinions and data contained in all publications are solely those of the individual author(s) and contributor(s) and not of MDPI and/or the editor(s). MDPI and/or the editor(s) disclaim responsibility for any injury to people or property resulting from any ideas, methods, instructions or products referred to in the content.